Large-Scale Circulation Features Associated with Decadal Variations of Tropical Cyclone Activity over the Central North Pacific

PAO-SHIN CHU

Department of Meteorology, School of Ocean and Earth Science and Technology, University of Hawaii at Manoa, Honolulu, Hawaii

(Manuscript received 20 February 2001, in final form 27 March 2002)

ABSTRACT

Tropical cyclone frequency in the central North Pacific (CNP) from 1966 to 2000 has exhibited decadal-scale variability. A statistical changepoint analysis reveals objectively that the shifts occur in 1982 and 1995, with fewer cyclones during the 1966–81 and 1995–2000 epochs and more during the 1982–94 epoch. A bootstrap resampling method is then applied to determine the frequency distribution of the mean annual cyclones for the 1966–81 and 1982–94 epochs, as well as to infer the confidence intervals of the observed mean and variance of cyclones for each epoch.

Large-scale environmental conditions conducive to cyclone incidences during the peak hurricane season (July–September) for the inactive (1966–81) and active (1982–94) epochs are investigated. A nonparametric Mann–Whitney test is used to investigate whether the differences in location between the two epochs are significant. In contrast to the first epoch, warmer sea surface temperatures, lower sea level pressure, stronger low-level anomalous cyclonic vorticity, reduced vertical wind shear, and increased total precipitable water covered a large domain of the tropical North Pacific in the second epoch. These changes in environmental conditions favor more cyclone incidences for the second epoch. Many of the aforementioned changes were already established prior to the peak season. In addition, atmospheric steering flows have changed remarkably in October and November so that tropical cyclones in the eastern North Pacific have a better chance to enter the CNP, and cyclones formed in the CNP are more likely to be steered through the western Hawaiian Islands in the second epoch.

1. Introduction

The tropical cyclone (TC) is one of the most destructive natural disasters that causes loss of lives and enormous property damages around the world. In the mainland United States, of the 10 costliest weather disasters in history, 6 of them were attributed to hurricanes, which are the strongest category of TC (more information available online at http://www.newstrench.com/03dislist/dislist.htm; also Elsner and Kara 1999). Information regarding these six hurricanes and their damage numbers can be found on the National Hurricane Center's Web site (http://www.nhc.noaa.gov/pastcost.html). In the North Pacific, Hawaii is also subject to TCs. In the past 20 years, the Hawaiian Islands were directly struck by two hurricanes: Iniki in September 1992 and Iwa in November 1982. Estimates of damages were about $2.5 billion for Iniki and $250 million for Iwa, a heavy toll for small islands with a population of 1.2 million.

Hurricane frequency in the North Atlantic has shown multidecadal variations. For instance, more hurricanes were observed during the late 1920s to the 1960s, followed by a relatively quiescent period from the 1970s to the early 1990s and by a recent surge since 1995 (Landsea et al. 1999; Elsner and Kara 1999; Goldenberg et al. 2001). Moreover, Gray and Sheaffer (1991) and Landsea et al. (1998) found that interannual variations in the seasonal activity of the Atlantic hurricanes are closely related to several environmental factors that influence tropospheric vertical wind shear. These factors include the El Niño–Southern Oscillation phenomenon, the Atlantic basin sea level pressure, sea surface temperatures in the tropical Atlantic, total precipitable water, and others. Through statistical analyses, Goldenberg and Shapiro (1996) also provided evidence that changes in the vertical wind shear are one of the most important factors in modulating interannual TC variability. In the Northwest Pacific, Chan and Shi (1996) noted a decrease in typhoon counts from the 1960s to the late 1970s, and an active period thereafter to 1994. Thus, during 1970–94, an approximately out-of-phase variation in TC frequency is found between the Northwest Pacific and North Atlantic.

For the central North Pacific (CNP), which is bordered by 140°W and the date line northward of the equator (Fig. 1), reliable TC records are shorter than for the Atlantic or Northwest Pacific. Nevertheless, decadal

Corresponding author address: Dr. Pao-Shin Chu, Department of Meteorology, School of Ocean and Earth Science and Technology, University of Hawaii at Manoa, 2525 Correa Road, Honolulu, HI 96822-2877.
E-mail: chu@soest.hawaii.edu

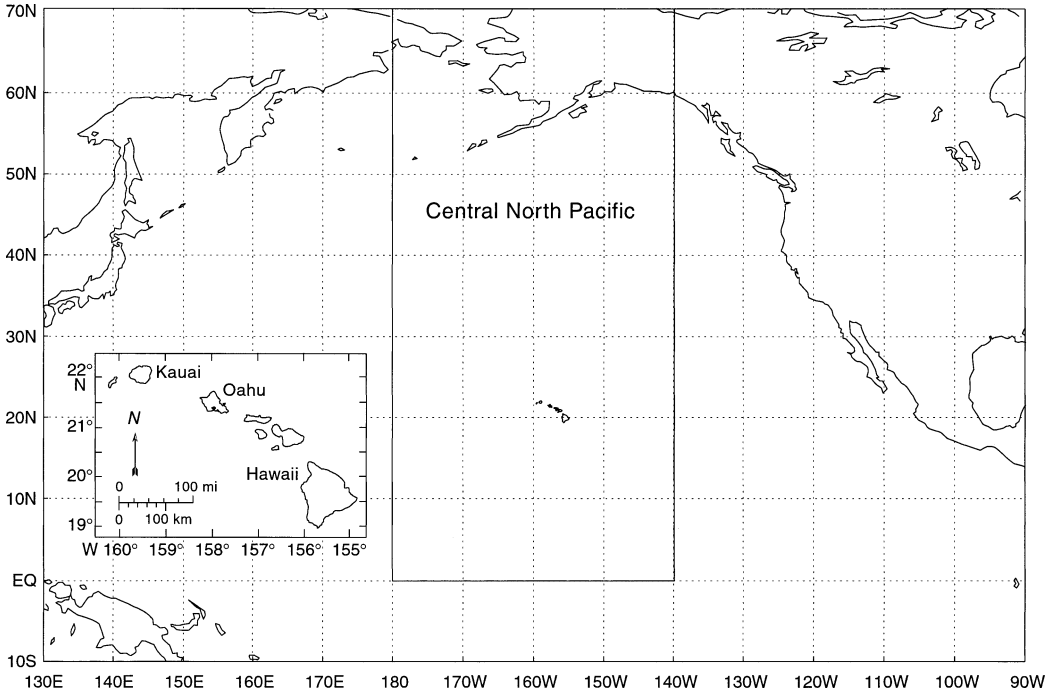

FIG. 1. Orientation map. The CNP is delineated in solid lines. Map of the major Hawaiian Islands is indicated in the inset.

variations in TC frequency are apparent since the mid-1960s, with fewer cyclones during the 1966–81 period and more during the recent 1982–97 period (Chu and Clark 1999). Particularly noteworthy is a shift in TC numbers in the early 1980s (Fig. 2). Specifically, the mean number of annual cyclones (tropical storms and hurricanes) increased from about two during the 1966–81 period to about four during the 1982–97 period. Concurrent with this increase in TC frequency from one period to another is a warming of the sea surface in the tropical Pacific and an enhancement of the area-averaged surface cyclonic vorticity to the south of Hawaii.

The present study expands on the Chu and Clark (1999) work by providing independent evidence that a major shift in TC series does occur in the early 1980s and by bringing a more complete physical understanding concerning decadal variations of TC activity over the CNP. We will first use a statistical analysis to ascertain the timing of change in TC time series. As will be seen later in section 3, the analysis objectively identifies two major epochs (1966–81 and 1982–94) with different TC activity. A bootstrap resampling technique will then be applied to distinguish TC statistics between the two epochs. Section 4 contrasts TC-related changes in large-scale environments over the North Pacific during the two different epochs. The environmental conditions include sea level pressure, sea surface temperature, low-level relative vorticity, tropospheric vertical wind shear, and precipitable water. The hypothesis we make is that large-scale slowly varying environmental conditions are different from one epoch to another in such a way that these conditions have become more favorable for cyclone activity during the second epoch. We will also investigate the epoch difference in the midtropospheric flow, which is generally thought to steer TC motions (Chan and Gray 1982). Finally, section 5 gives a summary and discussion.

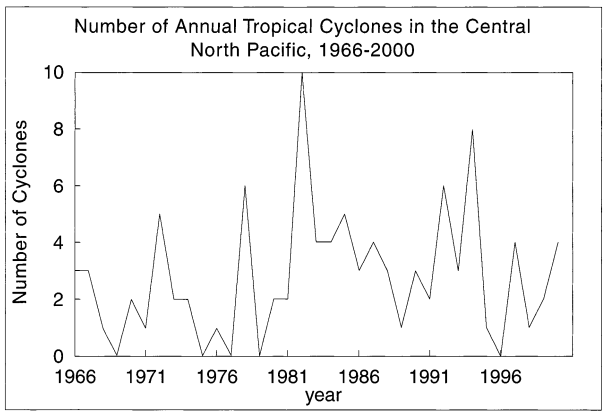

FIG. 2. Time series of TCs in the CNP from 1966 to 2000.

2. Data and data reliability

a. Data

As described in Chu and Wang (1997) and Chu and Clark (1999), the tropical storm (maximum sustained surface wind speeds between 17.5 and 33 m s^{-1}) and

hurricane (winds at least 33 m s^{-1}) records over the CNP at 6-h intervals from the National Hurricane Center's best track dataset are used (Brown and Leftwich 1982). The period of analysis is 1966–2000. The TC records prior to 1966 are thought to be less reliable because satellite observations were not in sufficient quantities. The domain of the CNP coincides with the area of responsibility of the Central Pacific Hurricane Center, an entity of the National Weather Service (NWS) in Honolulu, Hawaii.

Monthly mean sea level pressure (SLP), wind data at the 1000-, 850-, 500-, and 200-hPa levels, relative vorticity data at the 1000-hPa level, and total precipitable water are derived from the National Centers for Environmental Prediction–National Center for Atmospheric Research (NCEP–NCAR) reanalysis dataset (Kalnay et al. 1996). The NCEP–NCAR reanalysis project (hereafter referred to as reanalysis) uses a frozen assimilation technique to analyze past data and to eliminate noise due to different operational data assimilation schemes. The horizontal resolution of the reanalysis dataset is 2.5° latitude–longitude. In data-sparse regions, the forecast model forms the first guess. Tropospheric vertical wind shear (VWS) is given by

$$\mathrm{VWS} = [(u_{200\,\mathrm{hPa}} - u_{850\,\mathrm{hPa}})^2 + (v_{200\,\mathrm{hPa}} - v_{850\,\mathrm{hPa}})^2]^{1/2}, \quad (1)$$

where u and v denote the zonal and meridional wind components, respectively.

The monthly mean sea surface temperatures (SSTs) over the North Pacific are taken from Reynolds's reconstruction of the Comprehensive Ocean–Atmosphere Data Set, as detailed in Smith et al. (1996). All SST data are available on a 2° lat × 2° lon grid and are provided by the National Oceanic and Atmospheric Administration (NOAA) Climate Diagnostics Center in Boulder, Colorado.

b. Data reliability

While the reanalysis is one of the most used datasets in the climate community and constitutes the main database for this study, there are concerns about the quality of this dataset. Note that SLP and wind data are type-A variables in the reanalysis, meaning that they are strongly influenced by observations and are most reliable. To evaluate the reliability of the reanalysis data, a simple comparison between the monthly mean rawinsonde records in Hilo, Hawaii, and the closest grid point (20°N, 155°W) from the reanalysis dataset is made. Rawinsonde data come from the *Monthly Climatic Data for the World.* Correlation analysis is performed for the SLP and the zonal wind component for the months of July, August, and September, separately, over the period 1966–2000.

For SLP, the Pearson correlation coefficient between the station data and reanalysis is very high, reaching 0.978 for July, 0.86 for August, and 0.973 for September. For the zonal wind component at the 200-hPa level, the correlation coefficients are 0.85 for July, 0.83 for August, and 0.80 for September. Again, all these correlations are significant at the 1% level when Quenouille's (1952) method is used to account for the reduction of the effective number of degrees of freedom due to persistence (e.g., Hastenrath et al. 1984). At the lower troposphere (850 hPa), correlations of the zonal wind component between the two datasets are significant only for September (0.65); for the other two months the values are approximately 0.29. Compared to the 200-hPa level, lower correlation coefficients at 850 hPa are not unexpected because winds at this level in Hilo are influenced by local topographic effects.

Waliser et al. (1999) compared the NCEP–NCAR reanalysis wind with the in situ data (i.e., radiosonde, ship reports) for the period 1968–89. They noted that the configuration of the Hadley circulation is similar, but details differ between the reanalysis and observations. Relative to the in situ records, the southern Hadley cell is much weaker and the poleward boundary of the northern Hadley cell becomes more well defined in the reanalysis. However, in the area between the equator and 20°N, the large-scale circulation features are essentially the same for the reanalysis and in situ, lending support to the quality of the reanalysis wind data over the northern Tropics.

While the assimilation system remains unchanged in the reanalysis, the observing systems are evolving through time and can be classified into three phases (Kistler et al. 2001). The ''early'' phase spans from the 1940s to 1957, the ''modern rawinsonde'' phase from 1958 to 1978, and the ''modern satellite'' phase from 1979 to the present. Based on the anomaly correlation of the forecasting skill, Kistler et al. (2001) found that the impact of satellite or no satellite data is small in the Northern Hemisphere but large in the Southern Hemisphere. They further showed that in the monthly means, on which this study is based, the meridional wind component at 200 hPa over the CNP is virtually identical from the modern rawinsonde era to the modern satellite phase. Therefore, to a first order of approximation, the change in observing systems embodied in the reanalysis would have a minimum effect on tropospheric winds over the CNP.

For precipitable water, it is a type-B variable so that the model has a strong influence on the analysis. Compared with the blended dataset from the National Aeronautics and Space Administration's (NASA's) Water Vapor Project (NVAP), Trenberth and Guillemot (1998) found lower values in the Tropics in the reanalysis. One possibility for this dry bias is due to the use of the simplified Arakawa–Schubert convective parameterization scheme in the tropical atmosphere (e.g., Annamalai et al. 1999). Assuming that the moisture field in the reanalysis dataset has a consistent bias throughout the study period, this effect would be mitigated because

the purpose of this study is not to examine the absolute accuracy of the precipitable water data but rather to investigate the time-mean difference in this quantity between the two epochs.

3. Statistical analyses

a. Overall TC statistics

Two types of TCs appear in the CNP. The TC counts include storms that form within the CNP as well as those that form in the eastern North Pacific and propagate westward into the CNP. From 1966 to 2000, 98 TC occurrences were identified in the CNP. Out of these 98 TCs, 30 formed in the CNP (31%) and 68 moved into the region (69%). During this entire 35-yr period, the average number of annual TCs is 2.8.

The peak season of TCs in the CNP is July–September (JAS) when 85 TCs occurred. Immediately subsequent to JAS, the months of October–November (ON) also saw some activity, with nine TCs being observed in these two months. Prior to JAS, there is not a single TC occurrence on record in the months of February, May, and June. Unlike the eastern North Pacific where TCs do not occur in the cool season (McBride 1995), the CNP saw one TC occurrence in January, March, April, and December.

b. Changepoint analysis

Chu and Clark (1999) subjectively broke the entire 32-yr record of TC series (1966–97) in the CNP into two equal periods (1966–81 and 1982–97). This partition of the record was based on a steplike jump that occurred in 1982, and TC counts remained at a higher level of activity thereafter relative to the pre-1982 level. A question arises as to whether this partition is justifiable in an objective manner. In particular, is 1982 really a year when a major shift in TC frequency occurred? To answer this fundamental question, a statistical analysis is needed to pin down the exact time of decadal changes in TC incidences. Recently, Elsner et al. (2000) used a changepoint model to differentiate the active periods of the major Atlantic hurricane series from those of inactive periods during the last century. We will adopt this model to determine the temporal change in the rates of TC activity in the CNP.

Let X_i be the TC counts in year i and Y_i be $\log_{10}(X_i + 1)$. For an integer ℓ that varies from 2 to $m = n - 1$ where n is the total number of observations, the step variable is defined as

$$S_i(\ell) = \begin{cases} 0, & i < \ell \\ 1, & i \geq \ell. \end{cases} \tag{2}$$

A linear first-order regression model takes the form:

$$Y_i = \beta_0(\ell) + \beta_1(\ell)S_i(\ell) + \epsilon_i(\ell), \tag{3}$$

where $\beta_0(\ell)$ is the intercept, $\beta_1(\ell)$ is the slope, and $\epsilon_i(\ell)$ is the error or residual at Y_i for a fixed ℓ. Just as in the ordinary regression framework, the errors are assumed to be independent and identically distributed normal random variables with zero mean and constant variance. In reality, they may not be identically distributed because of the influence from a second or third change point. Likewise, the errors may also not be Gaussian. One may use a more sophisticated, nonparametric deviance reduction method for changepoint detection in the case of nonnormally distributed data (Venables and Ripley 1994). From (3), we define the t ratio as

$$t(\ell) = \hat{\beta}_1(\ell)/\text{se}[\hat{\beta}_1(\ell)], \tag{4}$$

where $\text{se}[\hat{\beta}_1(\ell)]$ is the estimated standard error of $\beta_1(\ell)$.

From (4), if the estimated slope is at least twice as large as its standard error, one would reject the null hypothesis (i.e., slope being zero) at the 5% significance level (Wilks 1995). Let $t(\ell_1) = \max\{|t(2)|, \ldots, |t(m)|\}$. If $t(\ell_1)$ is significant, one would conclude that the response Y_i has a changepoint at ℓ_1 with a rate $\beta_1(\ell_1)$. Once $t(\ell_1)$, the year of the first changepoint, is determined, this process is repeated with a new response variable $Y_i^* = Y_i - \hat{\beta}_1(\ell_1)S_i(\ell_1)$ and a second changepoint is then sought. This procedure is continued until all changepoints in the time series have been detected.

Making use of the above formula to the TC time series in the CNP, we found two significant changepoints, occurring in 1982 and 1995. Figure 3 shows the cumulative frequency of TCs as a function of time. Also plotted is a regression line for each period identified by the changepoint analysis. The first period is marked by an inactive TC regime from 1966 to 1981 with an average rate (regression slope) of 1.85 TCs yr^{-1}. This low TC activity is also seen in the time series plot of TC counts as revealed in Fig. 2. In Fig. 3, not surprisingly, the average rate increases to 3.45 TCs yr^{-1} during the second period that extends from 1982 to 1994. This is followed by another short, inactive period (1995–2000) that features a rate of 2.2 TCs yr^{-1}. Thus, from a purely

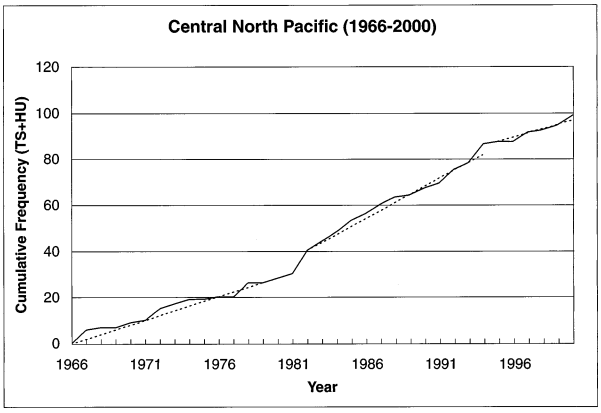

FIG. 3. Cumulative frequency of the annual number of TCs in the CNP from 1966 to 2000. Broken line denotes a simple regression line fitted to the periods: 1966–81, 1982–94, and 1995–2000.

TABLE 1. Mean and variance of the observed, annual number of TCs in the CNP for the two epochs, 1966–81 and 1982–94. The 95% confidence intervals for the mean and variance are obtained from the bootstrap resampling method.

Epoch	Mean of the annual number of cyclones from observations	The 95% confidence interval for the mean of the annual number of cyclones from bootstrap	Variance of the annual number of cyclones from observations	The 95% confidence interval for the variance of the annual number of cyclones from bootstrap
1966–81	1.88	(1.06, 2.75)	3.05	(0.92, 5.18)
1982–94	4.31	(3.15, 5.69)	6.06	(1.09, 10.81)

statistical analysis, we could identify objectively two changepoints with three periods in the TC series. Because the third period is short (only six years), we will concentrate on the first two epochs (1966–81 and 1982–94).

Having conducted the local test from the actual TC series, it remains interesting to evaluate the collective significance of multiple, independent local tests. Given a time series of 40 points, one of the computed t values would be expected to exceed the upper 2.5% critical value of the t distribution. Thus, a point is likely to be found significant when the 2.5% critical value is used, even if there is no real changepoint in the data. To account for the multiplicity effect, time series of TC records are scrambled using a random number generator. A similar changepoint analysis is performed for each resampled data and the number of local tests rejecting the null hypothesis is tabulated. This procedure is repeated for a large number of trials (1000 times). Results indicate an 87% chance that none or one changepoint could have occurred by repeated resampling of TC records. For detecting more than two changepoints in the resampling tests, the chance is rather rare, only 1.7%. Therefore, the probability is high that the observed two changepoints could not have occurred by random chance.

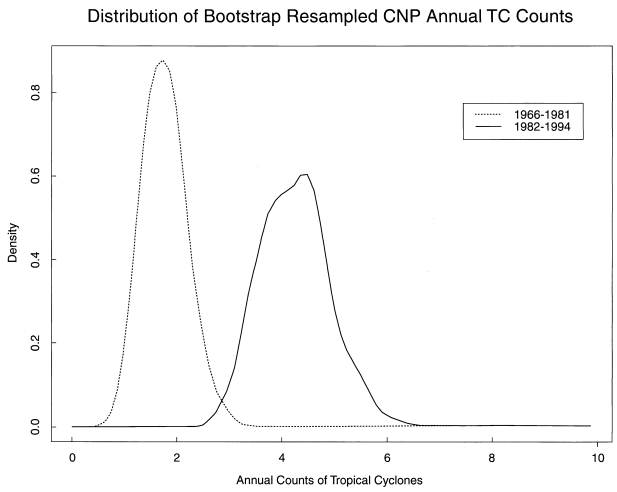

FIG. 4. Density distributions of the mean annual TC counts in the CNP for the 1966–81 and 1982–94 epochs as simulated by bootstrap.

c. Decadal TC statistics

In terms of decadal variations, 30 TCs occurred in the first epoch (1966–81) and nearly doubled the number (56) in the second (1982–94). In the first epoch, 9 TCs originated in the CNP (30%) and 21 TCs propagated into the CNP (70%). The second epoch features a similar proportion of TC frequencies as the first one, with 19 formed (34%) and 37 moved into the area of interest (66%). Thus, although the number of TC incidences between the two epochs is quite different, the percentage of named storms forming or entering the CNP remains similar from one epoch to another.

d. Bootstrap resampling

Because of the limited sample size in each epoch, a bootstrap resampling technique is applied to draw inferences about the TC statistics for each epoch. A bootstrap method operates on a construction of a large number of artificial data batches of the same size as the original dataset using sampling with replacement from the original data (e.g., Zwiers 1990). Chu and Wang (1997) used this method to simulate sampling distributions of the annual mean number of TCs in the vicinity of Hawaii during the El Niño and non–El Niño years. Bove et al. (1998) also used the bootstrap to estimate the confidence intervals of the probability of U.S. landfalling hurricanes given an El Niño or La Niña event. In this study, 2000 bootstrap realizations for each epoch are generated.

The mean number of annual TC counts for the early epoch is 1.88 from observations and its true value lies between 1.06 and 2.75 with 95% confidence as determined by the bootstrap technique (Table 1). In contrast, this mean value increases to more than 4.31 during the second epoch and the 95% confidence interval around the mean is (3.15, 5.69), a range that is broader than the first batch. Figure 4 shows the estimated sampling distribution of the mean TC count for each batch. While the distribution has a near-Gaussian shape for the earlier epoch, it becomes asymmetrical and more flat for the recent epoch. Compared to the first batch, larger variability is seen in the second batch. Indeed, the variance of the annual number of cyclones increases by nearly a factor of 2 from 3.05 during the early epoch to 6.06 during the recent epoch (Table 1).

e. A nonparametric test for the differences in location

The difference in the mean circulation between two epochs would naturally be tested for statistical significance. This is usually performed using a two-sample *t* test. One of the premises of the *t* test requires that two samples (i.e., data from two epochs) both possess the Gaussian distribution. Because of the small sample size of each epoch (16 and 13 each), it is not guaranteed that the two samples would fulfill the Gaussian distribution. Accordingly, a classic nonparametric test, known as the Mann–Whitney, for the differences in location (i.e., mean) between two epochs is used (e.g., Wilks 1995). To perform this test, the two data batches need to be pooled and ranked. The null hypothesis is that the two batches come from the same distribution.

Let U be the Mann–Whitney statistic:

$$U_1 = R_1 - \frac{n_1}{2}(n_1 + 1)$$

$$U_2 = R_2 - \frac{n_2}{2}(n_2 + 1), \tag{5}$$

where R_1 and R_2 denote the sum of the ranks held by the unit of batch 1 and 2 in the pooled distribution, respectively, and n_1 and n_2 are the sample size of batch 1 and 2, respectively. For moderately large sample size of batches, the null distribution of the U statistic follows approximately Gaussian with

$$\mu_U = \frac{n_1 n_2}{2} \quad \text{and}$$

$$\sigma_U = \left[\frac{n_1 n_2 (n_1 + n_2 + 1)}{12}\right]^{1/2}. \tag{6}$$

Once μ_U and σ_U are computed, the U statistic at each grid point is transformed into a standard Gaussian variable and is evaluated for its statistical significance.

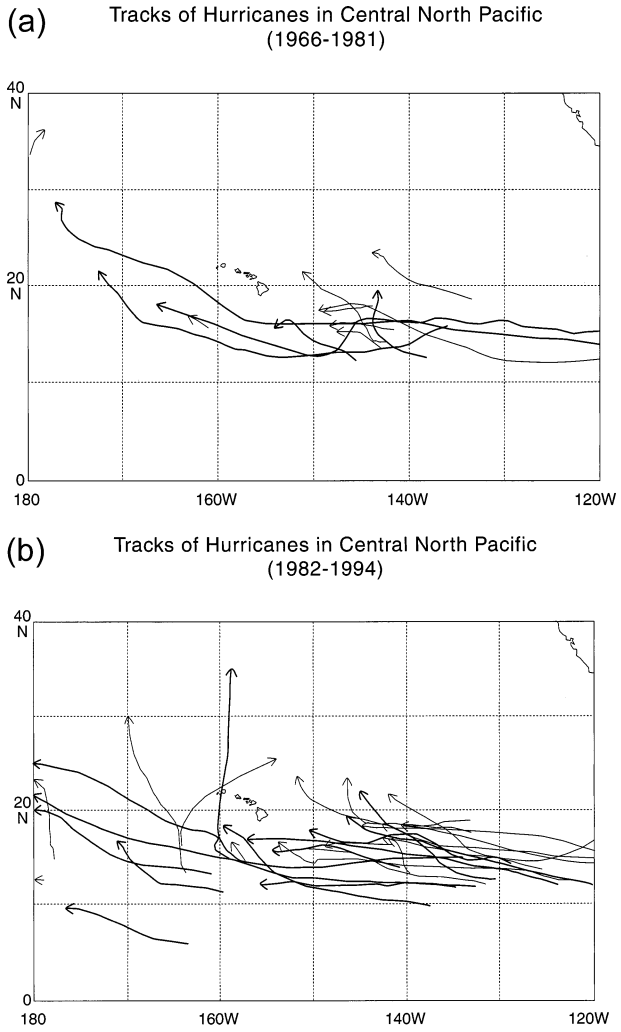

FIG. 5. Hurricane tracks in the CNP for the epoch (a) 1966–81 and (b) 1982–94. Heavy curves indicate hurricanes whose strength reached category three or above (sustained winds of at least 50 m s^{-1}) on the Saffir–Simpson scale.

4. Circulation changes

Because JAS is the most active season, maps of large-scale circulation differences for this season between the two epochs described in section 3 are analyzed. To illustrate the difference, the mean circulation from 1966 to 1981 will be subtracted from that in 1982–94. To help demonstrate the point that large-scale circulation changes are not only unique during the peak season, the difference maps in the preseason [May–June (MJ)] are also presented. Most hurricanes observed in the CNP either traversed or formed within the 10°–20°N latitudinal band (Fig. 5). For convenience, this band is called the major activity area (MAA).

a. Sea surface temperature (SST)

Figure 6a displays the SST difference map between 1982–94 and 1966–81 at the height of the hurricane season. Relative to the early epoch, a large area of positive and statistically significant difference in SST (warming of sea surface) covers the tropical Pacific and extends northeastward to the subtropical eastern North Pacific in the recent epoch. A band of negative difference in SST (cooling), with a southwest to northeast orientation, is located in the midlatitude ocean centered near 160°–140°W in the recent epoch. Relative to the first epoch, the area enclosed by the 26.5°C isotherm in the eastern/central MAA expands northward in the recent epoch. Note that the SST greater than 26.5°C is generally considered as the threshold for tropical cyclone formation. The SST pattern seen in JAS essentially persists through ON (not shown). While the tropical warming is maintained, the magnitude of midlatitude cooling decreases. The warmer SST in the Tropics in the recent epoch allows TCs to maintain their strength and induces low-level wind convergence. Warmer SSTs

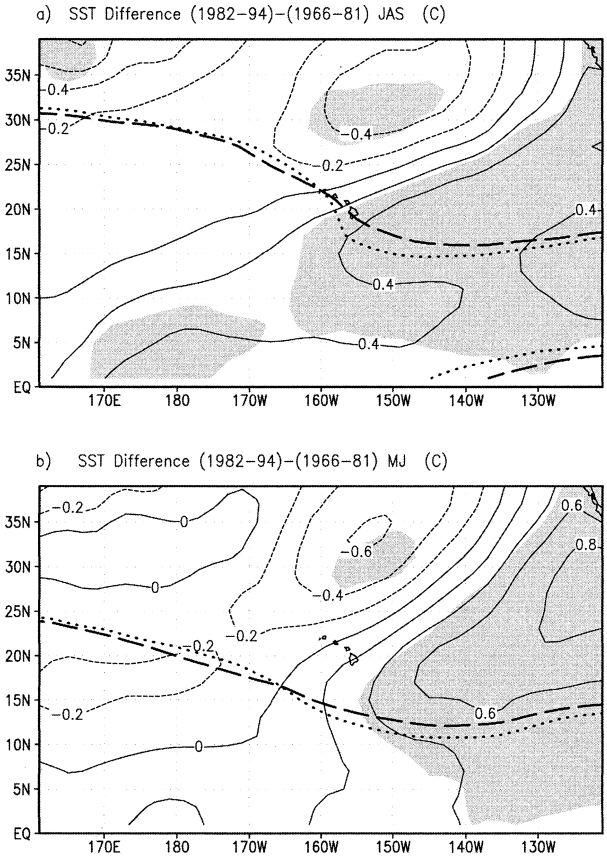

FIG. 6. SST difference (°C) between 1982–94 and 1966–81 over the North Pacific for (a) JAS and (b) MJ. Negative values are dashed. Contour interval is 0.2°C. The seasonal mean 26.5°C isotherm during 1982–94 and 1966–81 epochs is denoted by a heavy broken and dotted line, respectively. Shading indicates regions where the difference in the mean between two epochs is statistically significant at the 5% level.

are also seen in the preseason (MJ) in the recent epoch, particularly in the eastern North Pacific and the eastern tropical CNP (Fig. 6b).

b. Sea level pressure (SLP)

As TC is characterized by low pressure and cyclonic inflows near the surface, it is instructive to know how SLP varies from one epoch to another. Lower SLP is indicative of decreased subsidence and a weaker trade wind inversion that allows deeper convection to develop (Knaff 1997). As will be described later, given a deeper boundary layer, the entrainment of moist environmental air into the midtroposphere would be conducive to TC development. In addition, lower SLP in the Tropics may slacken the local pressure gradient, inducing weaker trade winds (Landsea et al. 1998). If the upper-level winds remain unchanged, weak easterly trades result in a reduction of vertical wind shear that favors TC formation.

Figure 7a displays the SLP differences between the two epochs in JAS. Interestingly, SLPs in the vicinity of Hawaii are lower and statistically significant in the recent epoch, with a value of −0.4 hPa. Although this difference seems to be small, it is considerable when viewed in the context of multiyear seasonal means. Higher SLPs are found mainly in the area equatorward of 10°N and in the midlatitude ocean centered near 143°W in the recent epoch. A question arises as to whether the lower pressures in the center of the study domain are merely an effect of TC or do they contribute to TC activity observed in the recent epoch. To help clarify this question, we have also analyzed the preseason SLP difference map. Note that there is no single occurrence of TC in May and June historically. As shown in Fig. 7b, the largest minimum difference occurs in the midlatitude ocean near 140°W, but lower SLPs extend equatorward to the eastern portion of the CNP where the SLP decrease is significant in the recent epoch. Because the pressure decrease persists from the preseason throughout the active season and covers a large area, lower SLPs as shown in Fig. 7a are suggestive as a contributing factor to the more active TCs in the recent epoch, rather than a response to TC activity.

c. Low-level relative vorticity

Climatologically, a band of low-level cyclonic vorticity stretches from 160°E to 120°W over the southern half of the MAA during the peak season (not shown). Anticyclonic relative vorticity dominates an area poleward of approximately 15°N. In Fig. 8a, a large portion of the MAA is dominated by positive differences in relative vorticity during the recent epoch, indicating either an increased cyclonic vorticity south of 15°N or a reduced anticyclonic vorticity north of 15°N. Also note that this positive difference is significant in two smaller areas, one to the south of Hawaii and the other near the date line.

Strong equatorial westerlies sometimes extend from the western Pacific to the central Pacific, as often observed during El Niño. For example, equatorial westerlies reached as far east as 155°W in November 1982 (J. Sadler 1986, personal communication). The presence of westerlies in low latitudes and easterly trade winds perturbs the climatological vorticity field, creating strong cyclonic shear and cyclonic relative vorticity in the MAA. Indeed, Chu (2002) found that the band of surface cyclonic vorticity in a large region of the tropical North Pacific in the El Niño composite is 2–3 times greater when compared to the corresponding La Niña composite. The cyclonic shear and vorticity are associated with the eastward displacement of the monsoon trough during El Niño years (Clark and Chu 2002). Presumably, it is this dynamical spinup, when coupled with other favorable environmental conditions, that is instrumental for more TC genesis in the CNP in the recent epoch. The positive difference in the relative vor-

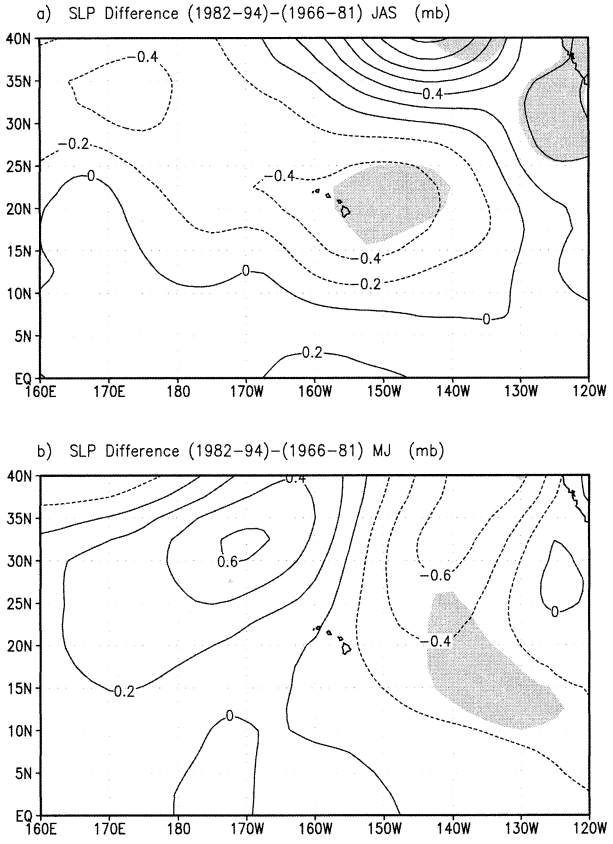

FIG. 7. Same as Fig. 6, but for SLP difference. Contour interval is 0.2 hPa.

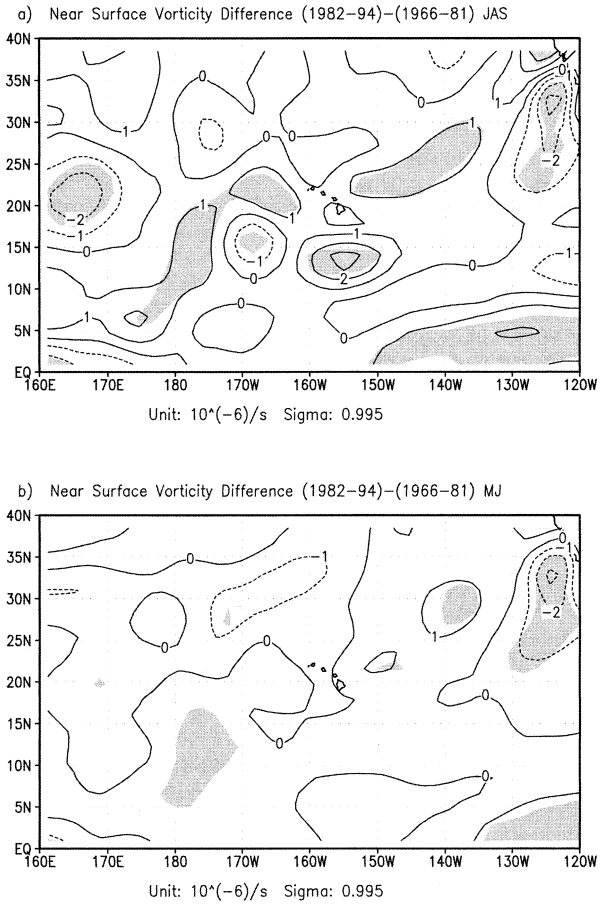

FIG. 8. Same as Fig. 6, but for the relative vorticity at 1000 hPa. Contour interval is 1×10^{-6} s^{-1}.

ticity is also seen in MJ in the recent epoch, although this difference is rather small (Fig. 8b).

d. Vertical wind shear (VWS)

In the CNP, persistent easterly trade winds at low levels combined with upper-level westerlies in summer and autumn to produce a strong climatological VWS. Strong VWS disrupts the organized deep convection (the so-called ventilation effect), which inhibits intensification of the incipient disturbance. Climatologically, the strong VWS, together with the absence of the monsoon trough in the MAA, keep the CNP from being a TC prone region. The difference in VWS between the two epochs is shown in Fig. 9a. A decrease in VWS is found in the MAA in the recent epoch. The meridional gradient in VWS decrease is very sharp with a local minimum as large as 4 m s^{-1} just to the south of Hawaii. This is also the area where the shear decrease in the recent epoch is statistically significant. It is interesting to note that the crucial vertical shear line, as represented by the 10 m s^{-1} isotach, shifts poleward in the recent epoch, implying a larger tropical area of weaker VWS in the recent epoch. Weaker VWS in the tropical and a portion of subtropical North Pacific also characterizes the preseason in the recent epoch (Fig. 9b). Thus, the weak VWS in the MAA persisted and intensified from the preseason to the peak season. VWS is a major factor in modulating the seasonal activity of the Atlantic hurricane (e.g., Gray and Sheaffer 1991; Goldenberg and Shapiro 1996; Landsea et al. 1998). Likewise, Clark and Chu (2002) noted a substantial reduction in the VWS equatorward of 16°N in a large area extending from 160° to 120°W in an El Niño composite when compared to a La Niña composite.

e. Total precipitable water (TPW)

It is known that midtropospheric moisture is directly related to tropical cyclogenesis and that drier atmosphere tends to suppress deep convection, and hence TCs. The importance of the atmospheric moisture for TC development is summarized by Knaff (1997) who noted: ''The entrainment of drier environmental air into developing TC systems results in less buoyancy for the system as well as diminished upper-level warming due to decreased release of latent heat.'' These two effects induced by drier entrainment air evidently inhibit TC formation. Collins and Mason (2000) found strong re-

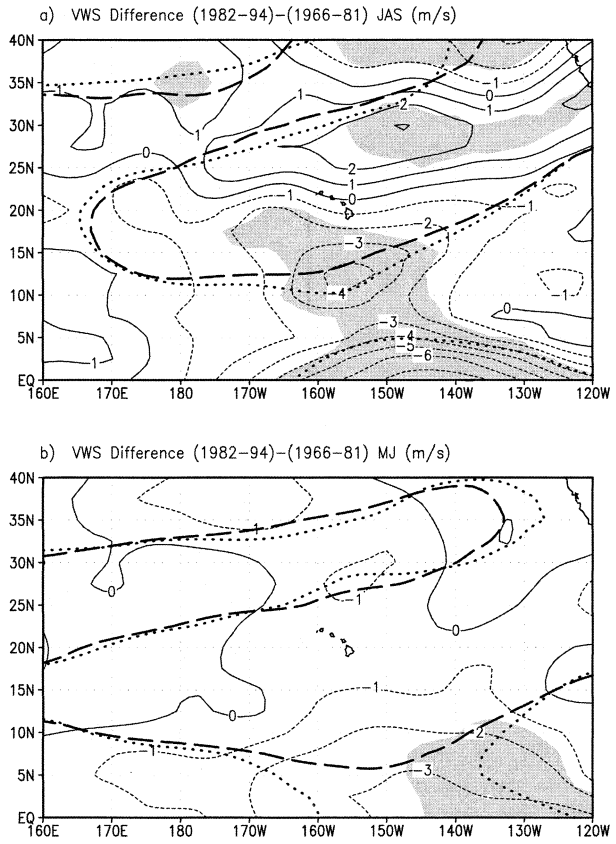

FIG. 9. Same as Fig. 6, but for the tropospheric VWS. Contour interval is 1 m s^{-1}. The seasonal mean 10 m s^{-1} vertical shear line during the 1982–94 and 1966–81 epochs is denoted by a heavy broken and dotted line, respectively.

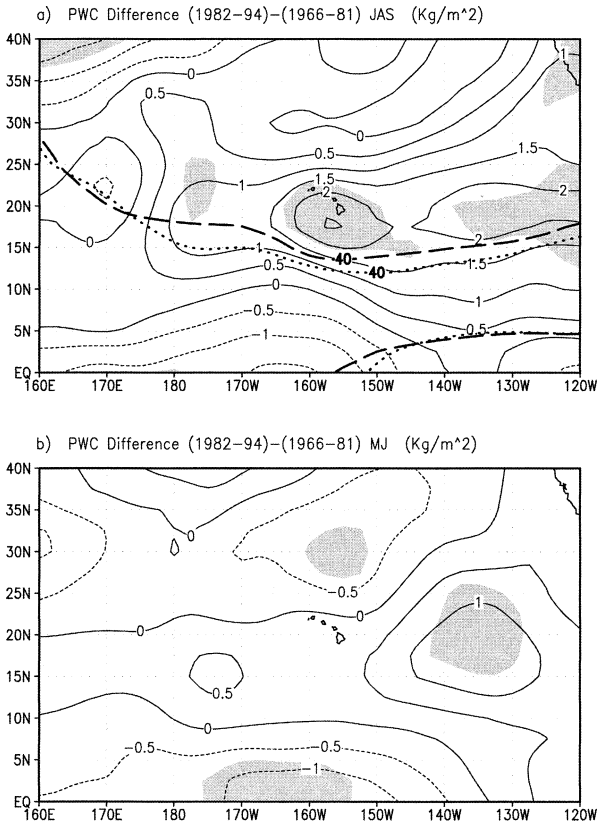

FIG. 10. Same as Fig. 6, but for the total precipitable water (TPW). Contour interval is 0.5 kg m^{-2}. The seasonal mean 40 kg m^{-2} TPW value during the 1982–94 and 1966–81 epochs is denoted by a heavy broken and dotted line, respectively. In May and Jun (b), TPW value is less than 40 kg m^{-2} and is not shown.

lationships between TC indices and some thermodynamic parameters (e.g., precipitable water) in the western portion of the eastern North Pacific (west of 116°W).

Figure 10a features the TPW difference for JAS between the two epochs. An increase in precipitable water is noted in a large band of the Tropics and subtropics in the recent epoch, and a statistically significant and maximum value as large as 2 kg m^{-2} is found surrounding the Hawaiian Islands. There is also an indication of a maximum value near 20°N that protrudes from the eastern North Pacific into the CNP. The increase in the TPW, or the depth of the moisture layer, is probably attributable to the increased moisture fluxes from the ocean surface as the SST becomes warmer in the recent epoch (Fig. 6a). Less subsidence drying could also account for more TPW in the recent epoch. The crucial moist TPW value, represented by the 40 kg m^{-2} isoline, moves farther poleward from the first to the second epoch, implying a larger area in the Tropics with deeper moisture layer in the recent epoch. In fact, the increase in the TPW in the MAA was already established in MJ and persisted as well as intensified through the peak season in the recent epoch (Fig. 10b). Interestingly, this increase in the moist layer depth is consistent with a warmer SST, a lower SLP, an increase in low-level cyclonic vorticity, and a reduction in VWS in the MAA in the recent epoch as seen previously.

f. Steering flows

Figure 11 displays the vector wind differences at 500 hPa for JAS and ON between the two epochs. The 500-hPa level is commonly identified as the steering level of TCs (e.g., Franklin et al. 1996). For JAS in the second epoch, the salient features include the easterly anomalies in the midlatitude eastern and central Pacific associated with an anomalous anticyclonic circulation in the higher latitudes of the North Pacific (Fig. 11a). An anomalously cyclonic circulation is found in lower latitudes extending from the western Pacific to the CNP where the difference in the zonal component of the steering flow is significant. Between approximately 15° and 20°N, weak easterly anomalies extend from 120°W westward. As seen in Fig. 11b, these easterlies become stronger and extend farther westward in ON.

By ON, the anomalous circulation changed quite noticeably from that in JAS, although none of the changes in the zonal wind component are statistically significant.

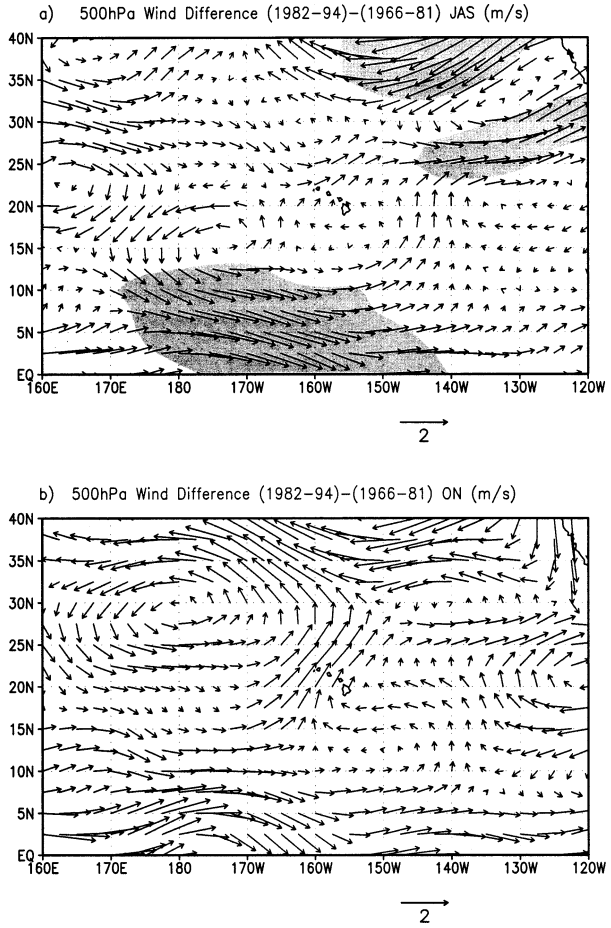

FIG. 11. 500-hPa wind vector differences (m s^{-1}) between 1966–81 and 1982–94 over the North Pacific for (a) JAS and (b) ON. Shading indicates regions where the difference in the zonal component of steering flow is statistically significant at the 5% level.

The anomalous anticyclonic cell in the eastern subtropical North Pacific appears to be well established in the recent epoch (Fig. 11b). Easterly anomalies on the southern flank of this cell, say at 17.5°N, can be observed from 120° to 157.5°W, suggesting TCs from the eastern North Pacific have a better chance of reaching the MAA of the CNP during the recent epoch. Also note that immediately south of Hawaii there is a small veering of wind anomalies from easterlies to southerlies. Taken together, there is a tendency for TCs to move from the eastern Pacific toward Hawaii in the second epoch. Strong easterlies prevail in the midlatitude North Pacific from approximately 130°W to 160°E, joined by an anomalous cyclonic cell to the northwest of Hawaii.

In the southwestern portion of the CNP (170°–160°W), southwesterly anomalies dominate the subtropics in the second epoch. This feature is different from that in JAS in which anomalously cyclonic circulation prevailed between the equator and 20°N in the CNP (Fig. 11a). Anomalous southwesterlies in Fig. 11b tend to steer TCs formed in the southwestern corner of the CNP toward the western Hawaiian Islands. One such example is Hurricane Iwa that has a northeastward track through Kauai, Hawaii (Fig. 1). The track of Iwa is shown in Chu and Wang (1998). The southwesterly anomalies in Fig. 11b appear to be connected with low-latitude westerlies from the western Pacific.

5. Summary and discussion

A statistical changepoint analysis applied to the time series of annual TC counts in the CNP provides objective guidance as to when there is a pronounced shift in the TC series. Results reveal that significant shifts occur in 1982 and 1995, and the entire period of 1966–2000 can be accordingly divided into three epochs of activity. The first epoch (1966–81) is marked by low TC activity as the rate of change is 1.85 TC yr^{-1}. This is in contrast to the second epoch (1982–94), which saw high activity with the rate of change being 3.45 TCs yr^{-1}. The third epoch, 1995–2000, is again inactive, with a rate of 2.2 TCs yr^{-1}. Because this epoch is short, the subsequent analyses focused on the first two epochs (1966–81 and 1982–94).

Based on this difference in annual rates between the aforementioned two epochs, a nonparametric bootstrap resampling technique is used to infer the frequency distribution of the mean annual cyclone incidences for each epoch. The bootstrap method operates by artificially generating data batches from a collection of each batch with replacement. Bootstrap sampling distributions of the mean annual cyclones between the two batches are quite different. The distribution for the early epoch is nearly Gaussian, but for the later epoch is relatively flat and asymmetrical. The mean number of cyclones per year during the second epoch is 4.31 and its 95% confidence interval estimated from bootstrap is between 3.15 and 5.69. This is in contrast to the first epoch when the mean of the annual incidence of the TC is 1.88 and the 95% confidence interval of the mean is between 1.06 and 2.75.

Large-scale environmental conditions instrumental for TC occurrences during the peak hurricane season between the two epochs are investigated. A statistical nonparametric test is applied to investigate whether the differences in location between these two epochs are different. In the CNP, most named storms traversed or formed within the latitudinal band between 10° and 20°N. For convenience, this band is called the major activity area. Relative to the first epoch, warmer SST, lower SLP, a reduced tropospheric vertical wind shear, an increase in the low-level cyclonic vorticity, and a deeper atmospheric moisture layer are found in the second epoch in the major activity area. While being statistically significant, these changes in environmental conditions favor more TCs observed in the CNP during 1982–94. Prior to the peak season, most of the aforementioned changes were already in existence in the second epoch. Given the fact that these changes are large

in spatial content and are precursory, they are contributing to, rather than an effect of, the more cyclones observed during the 1982–94.

Additionally, the 500-hPa flow changed dramatically, particularly in ON. In the second epoch, easterly anomalies dominate the eastern North Pacific and an area immediately to the south of the island of Hawaii. Furthermore, southwesterly anomalies are prevalent in the western Hawaiian Islands. Collectively, these changes in wind flows at the steering level imply that TCs from the eastern North Pacific have a better chance to penetrate to the CNP, and TCs formed in the western portion of the major activity area of the CNP are more likely to track through the western Hawaiian Islands during 1982–94.

It has been suggested by Kirtman and Schopf (1998), among others, that the decadal climate variability may play an important role in El Niño, the dominant interannual climate variation in the Tropics. The decadal variation may be regarded as a slowly varying mean climate state upon which El Niño evolves. Because the mean state of the Pacific SST has transitioned from a cold to a warm phase in the late 1970s (e.g., Trenberth and Hurrell 1994; Mantua et al. 1997), this warm decadal mode may have acted to influence the interannual variability, resulting in extraordinarily strong El Niño events as observed during 1982/83 and 1997/98 (e.g., Ware and Thomson 2000). In addition to the amplitude modulation, this warm decadal mode may also have resulted in a higher frequency of El Niño events during the last 20 years (e.g., Trenberth 1997; Ware and Thomson 2000).

Now the question is how the interplay between these two different climate forcings will affect decadal TC variability in the central North Pacific? Will they enhance or dilute decadal TC variations? During the second epoch when the Pacific mean climate state was warm, more cyclonic vorticity at the lower troposphere was observed to the south of Hawaii (Fig. 8a), contributing partly to more TC formation in the CNP. In the meantime, the decreased vertical wind shear and the increase in atmospheric water vapor in the major activity area during this epoch help TCs to maintain their life span and strength upon entering the CNP from east (Figs. 9 and 10). These changes in the large-scale circulation from one epoch to another were merely speculated in Chu and Clark (1999). Interestingly, many of the aforementioned changes, including the vertical wind shear and low-level vorticity, were also observed during the El Niño years (Chu 2002). Thus, as the large-scale dynamic and thermodynamic conditions have become more favorable for TC activity in the CNP during the second epoch, more TCs have developed or entered the CNP when El Niño became stronger or more frequent, broadly coinciding with a warm phase of the Pacific decadal SST mode. While the arguments put forth so far seem to be able to account for the active 1982–94 epoch, it is also puzzling to see the switch back to a quieter state of TC activity during 1995–2000 despite the presence of both a strong 1997/98 El Niño event and a warm decadal mode. This recent change in TC frequency calls for further investigations into its physical mechanisms and for possibly development of a method for TC prediction on a decadal basis.

Acknowledgments. Maria Rakotondrafara and Wendy Chen performed the data analyses. Constructive criticisms from Chris Landsea, Francis Zwiers, and an anonymous reviewer helped to greatly improve the presentation of this paper. Thanks also go to Jim Elsner and T. Schroeder for their comments, to Di Henderson for technical editing, and to the First Insurance of Hawaii and Guy–Carpenter Reinsurance Companies for their support.

REFERENCES

Annamalai, H., J. M. Slingo, K. R. Sperber, and K. Hodges, 1999: The mean evolution and variability of the Asian summer monsoon: Comparison of ECMWF and NCEP–NCAR reanalyses. *Mon. Wea. Rev.,* **127,** 1157–1186.

Bove, M. C., J. B. Elsner, C. W. Landsea, X. Niu, and J. J. O'Brien, 1998: Effect of El Niño on U.S. landfalling hurricanes, Revisited. *Bull. Amer. Meteor. Soc.,* **79,** 2477–2482.

Brown, G. M., and P. W. Leftwich Jr., 1982: A compilation of eastern and central North Pacific tropical cyclone data. NOAA Tech. Memo. NWS NHC 16, Miami, FL, 15 pp.

Chan, J. C. L., and W. M. Gray, 1982: Tropical cyclone movement and surrounding flow relationships. *Mon. Wea. Rev.,* **110,** 1354–1374.

——, and J.-E. Shi, 1996: Long-term trends and interannual variability in tropical cyclone activity over the western North Pacific. *Geophys. Res. Lett.,* **23,** 2765–2767.

Chu, P.-S., 2002: ENSO and tropical cyclone activity. *Hurricanes and Typhoons: Past, Present, and Potential,* R. J. Murnane and K. B. Liu, Eds., Columbia University Press, in press.

——, and J. Wang, 1997: Tropical cyclone occurrences in the vicinity of Hawaii: Are the differences between El Niño and non-El Niño years significant? *J. Climate,* **10,** 2683–2689.

——, and ——, 1998: Modeling return periods of tropical cyclone intensities in the vicinity of Hawaii. *J. Appl. Meteor.,* **37,** 951–960.

——, and J. D. Clark, 1999: Decadal variations of tropical cyclone activity over the central North Pacific. *Bull. Amer. Meteor. Soc.,* **80,** 1875–1881.

Clark, J. D., and P.-S. Chu, 2002: Interannual variation of tropical cyclone activity over the central North Pacific. *J. Meteor. Soc. Japan,* **80,** 403–418.

Collins, J. M. and I. M. Mason, 2000: Local environmental conditions related to seasonal tropical cyclone activity in the northeast Pacific basin. *Geophys. Res. Lett.,* **27,** 3881–3884.

Elsner, J. B., and A. B. Kara, 1999: *Hurricanes of North Atlantic: Climate and Society.* Oxford University Press, 488 pp.

——, T. Jagger, and X.-F. Niu, 2000: Changes in the rates of North Atlantic major hurricane activity during the 20th century. *Geophys. Res. Lett.,* **27,** 1743–1746.

Franklin, J. L., S. E. Feuer, J. Kaplan, and S. D. Aberson, 1996: Tropical cyclone motion and surrounding flow relationships: Searching for beta gyres in omega dropsonde datasets. *Mon. Wea. Rev.,* **124,** 64–84.

Goldenberg, S. B., and L. J. Shapiro, 1996: Physical mechanisms for the association of El Niño and West Africa rainfall with Atlantic major hurricane activity. *J. Climate,* **9,** 1169–1187.

——, C. W. Landsea, A. M. Mestas-Nunez, and W. M. Gray, 2001:

The recent increase in Atlantic hurricane activity: Causes and implications. *Science,* **293,** 474–479.
Gray, W. M., and J. D. Sheaffer, 1991: El Niño and QBO influences on tropical cyclone activity. *Teleconnections Linking Worldwide Climate Anomalies,* M. H. Glantz, R. W. Katz, and N. Nicholls, Eds., Cambridge University Press, 257–284.
Hastenrath, S., M.-C. Wu, and P.-S. Chu, 1984: Towards the monitoring and prediction of northeast Brazil droughts. *Quart. J. Roy. Meteor. Soc.,* **110,** 411–425.
Kalnay, E., and Coauthors, 1996: The NCEP/NCAR 40-Year Reanalysis Project. *Bull. Amer. Meteor. Soc.,* **77,** 437–471.
Kirtman, B. P., and P. S. Schopf, 1998: Decadal variability in ENSO predictability and prediction. *J. Climate,* **11,** 2804–2822.
Kistler, R., and Coauthors, 2001: The NCEP–NCAR 50-Year Reanalysis: Monthly means CD-ROM and documentation. *Bull. Amer. Meteor. Soc.,* **82,** 247–267.
Knaff, J. A., 1997: Implications of summertime sea level pressure anomalies in the tropical Atlantic region. *J. Climate,* **10,** 789–804.
Landsea, C. W., G. D. Bell, W. M. Gary, and S. B. Goldenberg, 1998: The extremely active 1995 Atlantic hurricane season: Environmental conditions and verification of seasonal forecasts. *Mon. Wea. Rev.,* **126,** 1174–1193.
——, R. A. Pielke, A. M. Mestas-Nunez, and J. A. Knaff, 1999: Atlantic basin hurricanes: Indices of climatic changes. *Climatic Change,* **42,** 89–129.
Mantua, N. J., S. R. Hare, Y. Zhang, J. M. Wallace, and R. C. Francis, 1997: A Pacific interdecadal oscillation with impacts on salmon production. *Bull. Amer. Meteor. Soc.,* **78,** 1069–1079.
McBride, J. L., 1995: Tropical cyclone formation. *Global Perspectives on Tropical Cyclones,* R. L. Elsberry, Ed., WMO Tech. Document 693, 63–105.
Quenouille, M. A., 1952: *Associated Measurements.* Butterworths, 242 pp.
Smith, T. M., R. W. Reynolds, R. E. Livezey, and D. C. Stokes, 1996: Reconstruction of historical sea surface temperatures using empirical orthogonal functions. *J. Climate,* **9,** 1403–1420.
Trenberth, K. E., 1997: The definition of El Niño. *Bull. Amer. Meteor. Soc.,* **78,** 2771–2777.
——, and J. W. Hurrell, 1994: Decadal atmosphere–ocean variations in the Pacific. *Climate Dyn.,* **9,** 303–319.
——, and C. J. Guillemot, 1998: Evaluation of the atmospheric moisture and hydrological cycle in the NCEP/NCAR reanalysis. *Climate Dyn.,* **14,** 213–231.
Venables, W. N., and B. D. Ripley, 1994: *Modern Applied Statistics with S-Plus.* Springer, 548 pp.
Waliser, D. E., Z. Shi, J. Lanzante, and A. Oort, 1999: The Hadley circulation: Assessing reanalysis and sparse in-situ estimates. *Climate Dyn.,* **15,** 719–735.
Ware, D. M., and R. E. Thomson, 2000: Interannual to multidecadal timescale climate variations in the northeast Pacific. *J. Climate,* **13,** 3209–3220.
Wilks, D. S., 1995: *Statistical Methods in the Atmospheric Sciences.* Academic Press, 467 pp.
Zwiers, F. W., 1990: The effect of serial correlation on statistical inference made with resampling procedures. *J. Climate,* **3,** 1452–1461.